Mater. Res. Soc. Proc. Vol. 563, 1999 Symposium M: Material Reliability in Microelectronics IX

ACOUSTIC EMISSION ANALYSIS OF FRACTURE EVENTS IN Cu FILMS WITH W OVERLAYERS

Alex A. Volinsky and William W. Gerberich
University of Minnesota, Dept. of Chem. Engineering and Materials Science, Minneapolis, MN, 55455, volinsky@cems.umn.edu

ABSTRACT

Indentation-induced delamination of thin films provides the basis for adhesion calculations. In the case of ductile Cu films plastic deformation usually prevents a film from debonding from the substrate. Deadhesion is facilitated by the use of a hard W superlayer, which promotes indenter-induced Cu film failure, increasing the delamination area by an order of magnitude. Radial as well as annular cracking acts like a secondary mechanism in the strain energy release, and can be resolved from excursions on the load-displacement curves. For the thicker Cu films no excursions were observed, though radial cracking took place. It is important to identify fracture events as they occur in order to understand the system behavior and accurately apply the analysis. An acoustic emission signal is used to detect both the magnitude and the type of fracture events in thin Cu films. For the films of different thickness from 40 nm to 3 microns the corresponding interfacial fracture energy ranged from 0.2 to over 100 J/m^2. Limits of plastic energy dissipation are determined with the lower limit, the true work of adhesion, being associated with a dislocation emission criterion. Crack arrest marks were found upon the blister removal, and are proposed to represent the shape of the crack tip. Total acoustic emission energy was found to be inversely proportional to the strain energy release rate.

INTRODUCTION

Acoustic emission (AE) is a very powerful method for examining the behavior of materials deforming under stress. This covers fracture, yielding, fatigue, corrosion, creep, etc. in bulk materials, including composites [1]. Several researchers have tried to employ AE for the detection of yielding and fracture events in different thin film systems [2-5]. In the present study, we consider indentation-induced delamination in the superlayer structure (Figure 1).

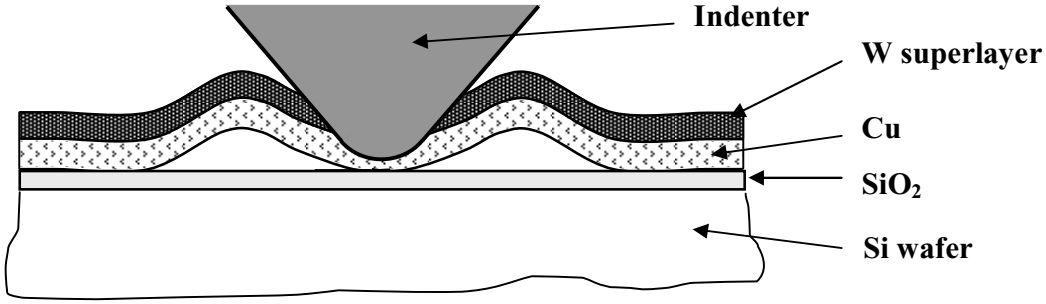

Figure 1. Schematic of the superlayer indentation.

A superlayer indentation method is used for thin film adhesion determination. In the case of ductile or strongly adhered films, it is often impossible to cause film delamination from the substrate by means of indentation. Ductile thin films cannot store enough strain energy necessary for crack initiation/propagation. Deposition of a hard film, capable of storing sufficient amounts

of elastic energy over the film of interest, can result in multilayer debonding, producing much larger delamination radii.

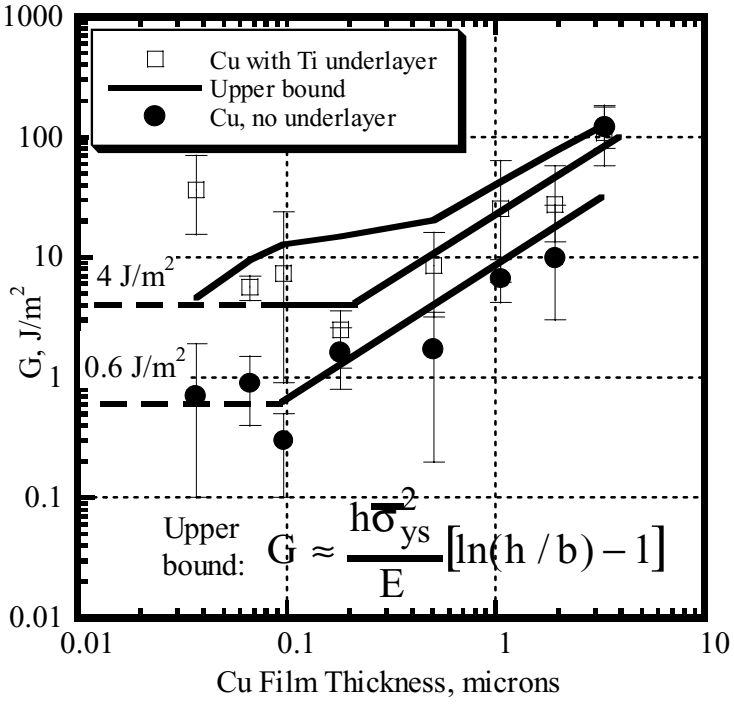

Figure 2. Cu thin film adhesion.

Copper thin film adhesion was shown to increase with the film thickness and with the addition of a 10 nm thin Ti underlayer due to the higher plastic energy dissipation at the crack tip (Figure 2) [6-8]. For the lower film thicknesses (up to 100 nm) without the Ti underlayer the plastic energy dissipation in the Cu film was found to be nil. Here, the strain energy release rate is proposed to be twice the true work of adhesion with an average of 0.6 J/m^2 being measured.

EXPERIMENTAL PROCEDURE

All thin film processing was conducted in a class 10 clean room environment. Silicon <100> wafers (100 mm in diameter, 0.5 mm thick) were thermally oxidized at 1100 °C in steam to grow 1.5 μm of SiO_2. Oxide thickness was measured with a Nanoscope Ellipsometer. The Cu films were deposited in a 2400 Perkin-Elmer sputtering apparatus. During sputtering, the base pressure of the system was 1 μTorr, and the Ar pressure was 12 mTorr. Substrate table rotation was used to achieve uniform Cu film thickness and nanostructure. Tungsten superlayers were deposited at 7 mTorr Ar pressure to achieve 300 MPa compressive residual stress in the W layer. Cu films were under 300 MPa residual tensile stress. The maximum temperature during film deposition reached 100 °C after which the system was cooled for one hour without breaking the vacuum in order to prevent film oxidation.

For all the experiments, samples were bonded with cyanoacrylate to a acoustic emission sensor from Physical Acoustics Corporation. All samples were indented with the IBM Micromechanical Tester (MMT) [9] and the AE waves were recorded with the MISTRAS 2001 system by Physical Acoustics Corp. A schematic of the experimental setup is shown in Figure 3.

The MISTRAS 2001 is a fully digital, computerized, acoustic emission system that performs waveform and signal measurements. The actual waves of the signals above a given threshold were recorded automatically during the indentation test. The preamplifier with a built-in 100-300 kHz filter was set to a 60 dB gain, and the signal was collected at a 10 MHz rate.

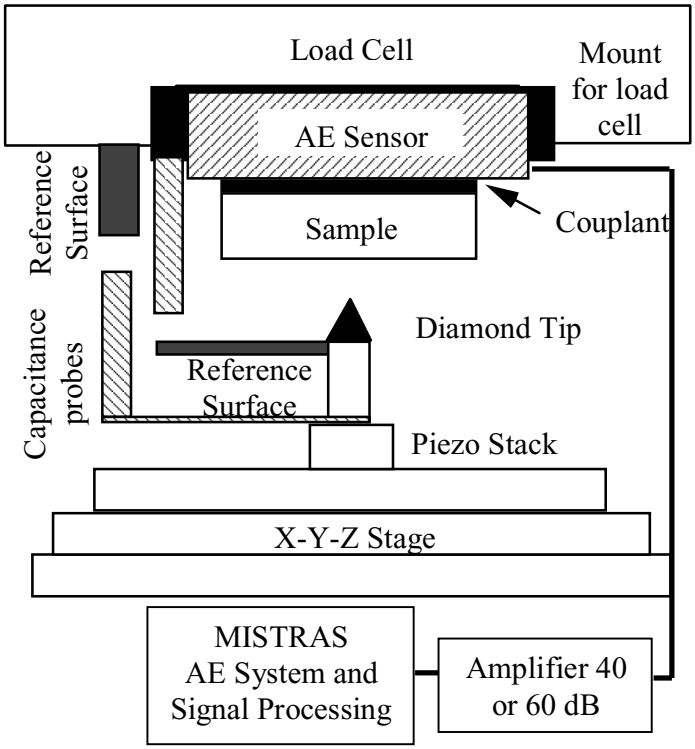

Figure 3. Schematic of experimental setup.

ACOUSTIC EMISSION DURING THIN FILM NANOINDENTATION

Acoustic emission events for an indentation into 120 nm thick Cu film with Ti underlayer are presented in Figure 4.

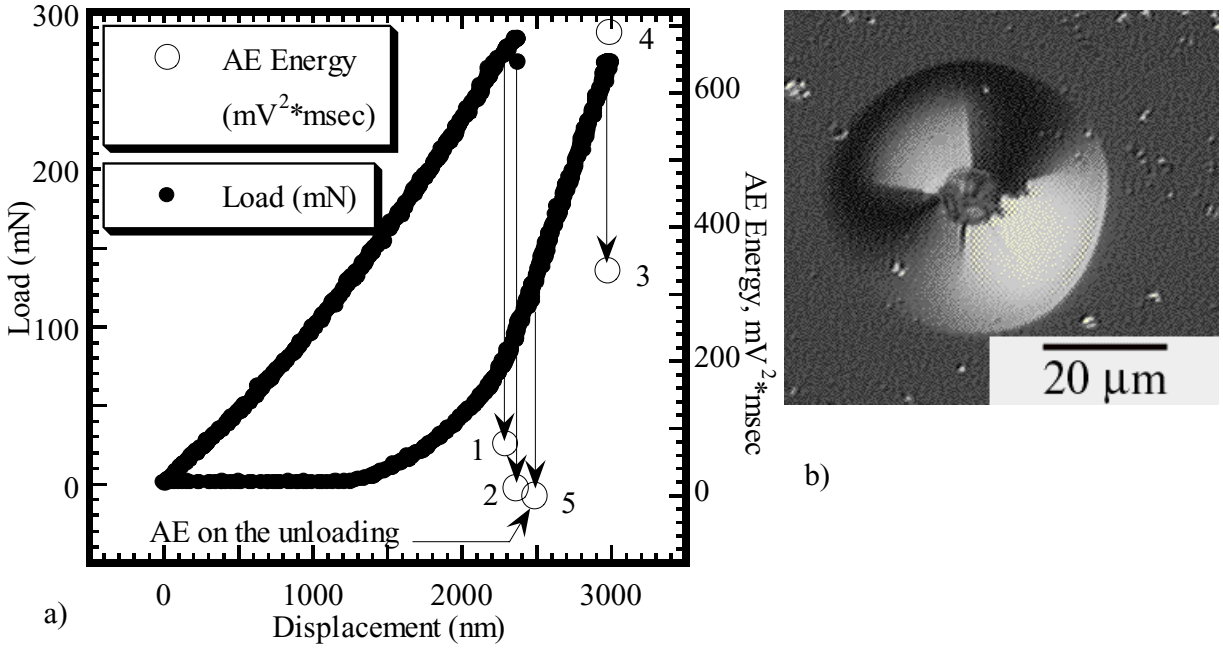

Figure 4. a) Load-displacement curve and acoustic emission events for a Ti/Cu/W indentation; b) Nomarski optical image of the corresponding blister.

As in the previous studies [6], excursions on the load-displacement curves were observed above a certain load level. For the indentation shown in Figure 4, the load excursion occurs during a constant load hold and four acoustic emission events of different magnitudes are associated with the excursion. One small AE event was observed on the unloading. The actual AE signals are shown in Figure 5. It is clearly seen that the rise time is much higher for the maximum amplitude signal than for the rest of them. The rise time is not truly indicative of the lifetime of the event, but is a combination of the original signal, its reflections and the piezoelectric detector response. For a fixed energy level, the rate at which the energy is released by a defect in a given system is proportional to the rise time [11]. Here, we find the total acoustic emission energy to be proportional to the rise time. For both film systems, with and without Ti underlayer, the total AE energy increases with the rise time (Figure 6).

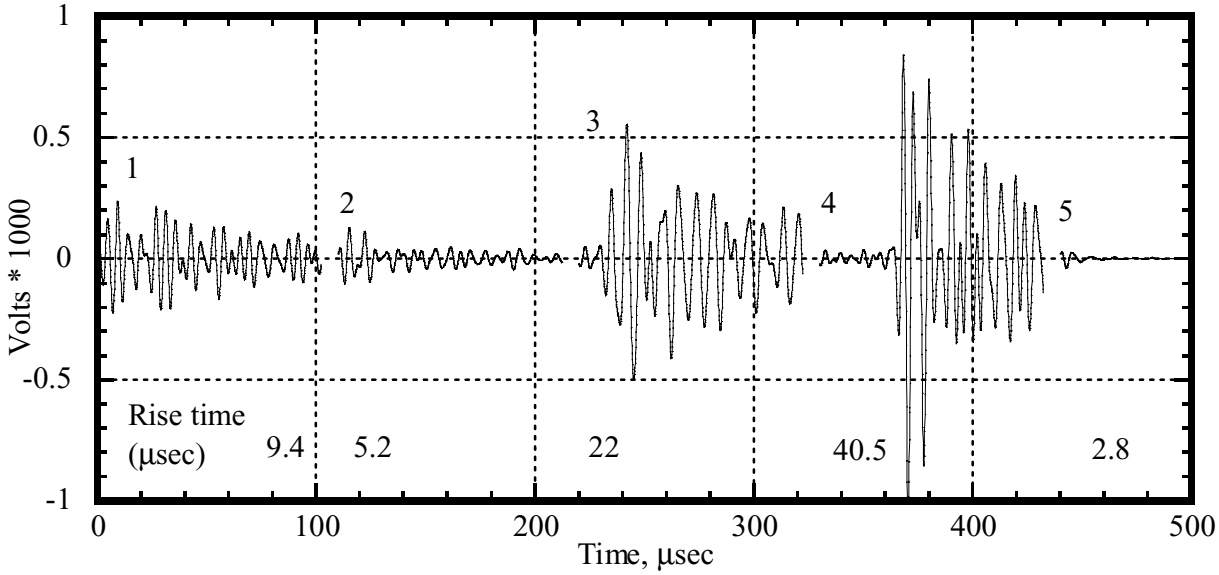

Figure 5. Acoustic emission signals during Ti/Cu/W indentation. Signals are put on the same time scale.

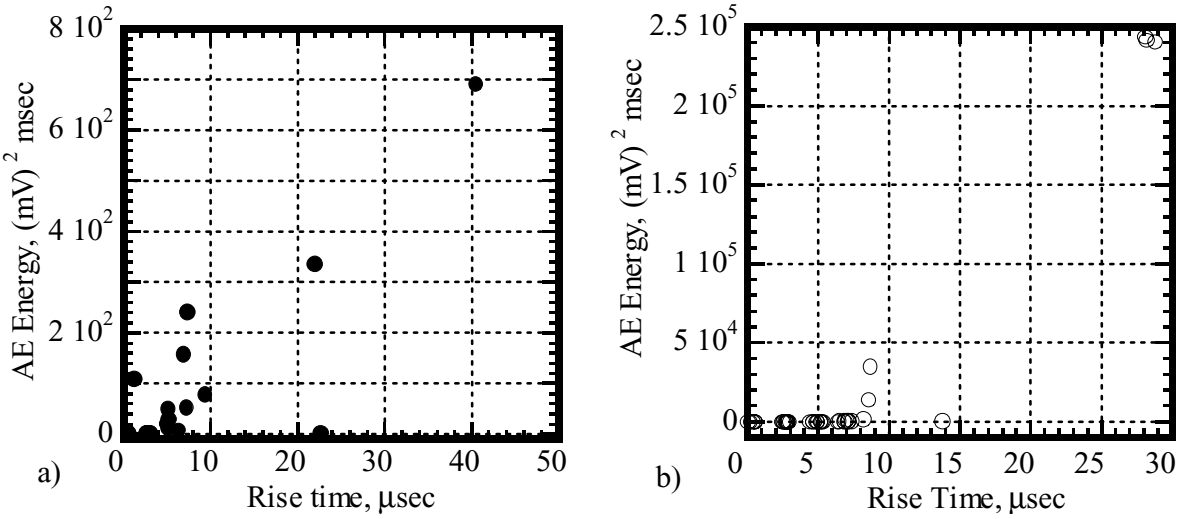

Figure 6. Total AE energy: a) Ti underlayer; b) no Ti underlayer.

As expected, the amount of emitted AE energy increased with the load and thus the blister size (Figure 7a). What we find interesting, though, is that the strain energy release rate, the measure of thin film adhesion, decreases with the total acoustic emission energy emitted. This result is the opposite of what was observed in previous studies on single crystal systems, where dislocation activity governs acoustic emission mostly [5]. For thin films systems the situation can be different, since the amount of the released acoustic energy is proportional to the crack area [12], and depends on the crack growth rate. In less well-adhered areas of the film (low G values) more acoustic energy could be released if delamination occurs in a single event. Alternatively, for the well-adhered areas of the film (high G values) much of the cracking is by subcritical crack growth in such small increments as to be below our detection threshold.

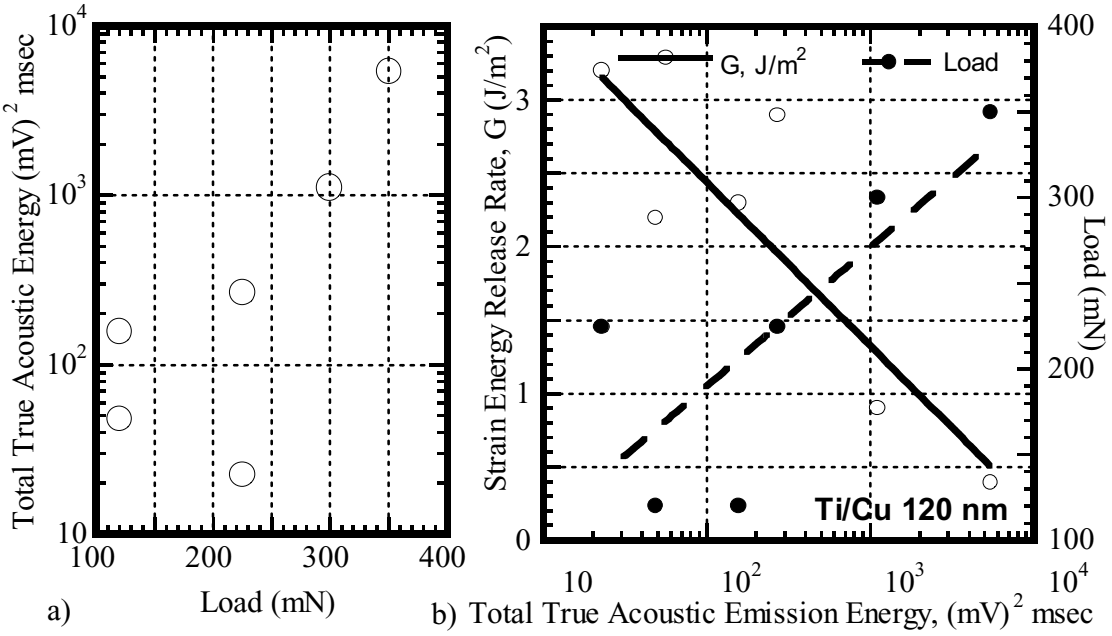

Figure 7. a) Total AE energy; b) Strain energy release rate for the films with Ti underlayer.

In order to determine that the collected acoustic emission signals are not associated with substrate cracking due to the high normal loads, a plane Cu film without the W superlayer was also indented. For a given load, the distance between the indenter tip and a film/substrate interface is much lower in this case, compared with the W superlayer. Figure 8 shows the total true acoustic emission energy for an uncovered Cu film, and the superlayer structure, with and without the Ti adhesion-promoting underlayer. The magnitude of the total acoustic energy is much higher for the films without Ti underlayer. For the same film thickness Ti increases Cu film adhesion by an order of magnitude [6], thus for a given load much smaller blister radii will result, emitting less acoustic energy.

The AE is low for the low load indents into the Cu film (up to 50 mN). It increases drastically at a 100 mN due to blister formation and substrate cracking [13]. In the case of a W superlayer the indenter does not penetrate the substrate as deep. In this case, the normal loads are not high enough to produce substrate radial cracking. In order to check this blisters were removed so that the SiO_2 surface was exposed for examination.

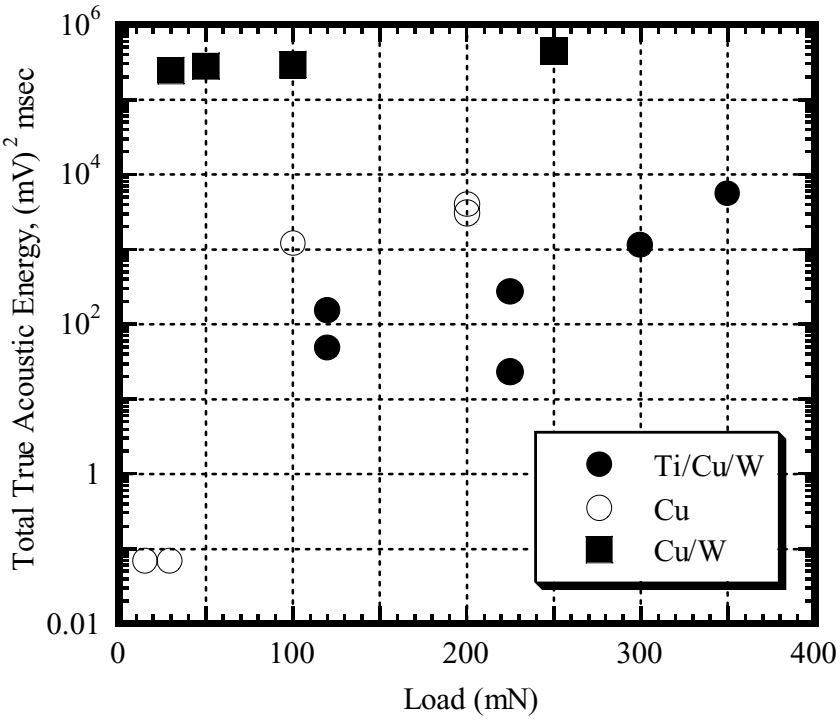

Figure 8. Total true acoustic emission energy as a function of load.

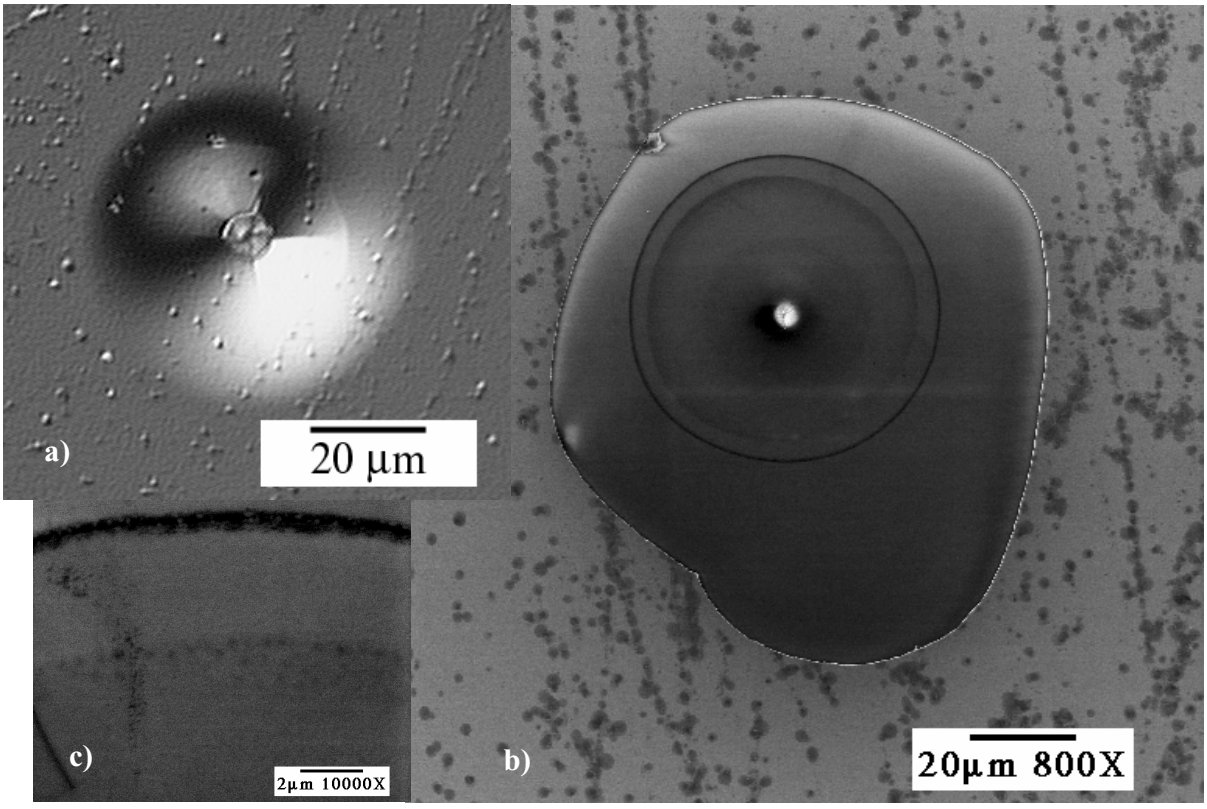

Figure 9. a) Optical image of a blister; b) SEM image of the area underneath the removed blister in a); c) SEM image of a crack arrest mark.

"INSIDE THE BLISTER"

Several blisters were removed with adhesive tape. Figure 9a shows a Nomarski contrast optical image of the original blister of a Cu film without a Ti underlayer. The area under the removed blister is presented with the SEM image in Figure 9b. The crack propagated further than the original blister size when the tape was removed. No substrate cracking was observed.

In order to determine whether the crack propagated at the SiO_2/Cu interface, Auger electron surface analysis was performed. Four 100 μm^2 regions were scanned in the delaminated area. The elemental concentration profile is shown in Figure 10. There is a high surface concentration of oxygen and carbon due to contamination and the presence of oxygen in the SiO_2. The oxygen concentration drops from 60 to 40 % upon moving out of the delamination zone to the W surface. The tungsten concentration changes accordingly. A small, almost indistinguishable Cu concentration compared to background inside the blister suggests that the Cu film is totally removed during blister formation. An increase in the carbon concentration outside of the delaminated area can be explained by hydrocarbon surface contamination.

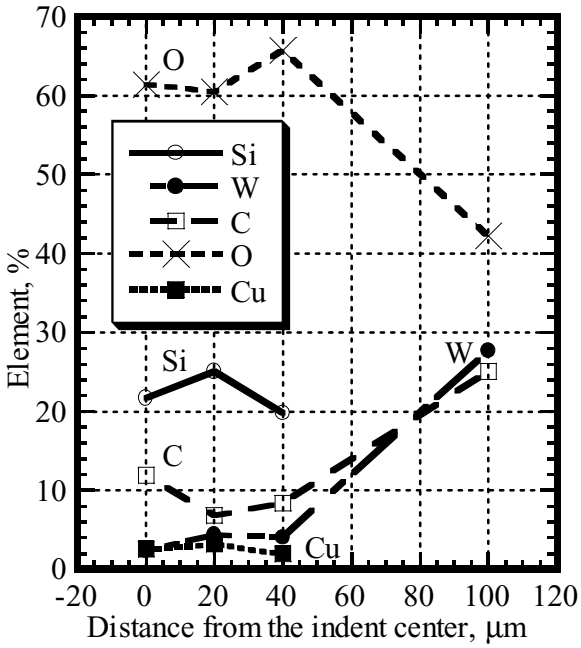

Figure 10. Element concentration profile.

Scanning electron microscopy also showed a circle that corresponds to the original blister size in diameter. Two distinct circular marks are clearly seen on the SEM higher magnification image in Figure 9c. We denote those as crack arrest marks. Atomic force microscopy was performed to measure the feature geometry. Feature width is 1 μm, and it's height ranges from 5 to 15 nm. Contact and deflection AFM images of the blister mark are shown in Figure 11.

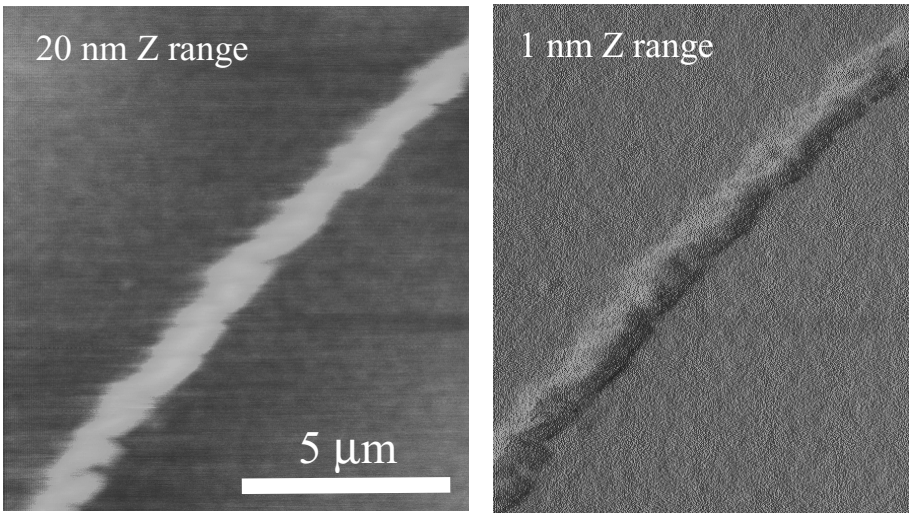

Figure 11. a) Contact and b) deflection AFM images of the crack arrest mark.

We believe that the crack arrest mark is formed by crushed W and/or SiO_2 debris during the indentation. It is also possible that due to radial cracking exposure to laboratory air allowed moisture, hydrocarbons and surface debris to be sucked into the blister area. Whatever the source, relatively mobile moisture, hydrocarbons and small debris particles were sucked into the crack tip leaving the fiducial mark detected in Figure 9b. This is identically analogous to the method used in the early days of the E24 subcommittee on fracture toughness testing where it was desired to mark the extent of slow crack growth prior to rapid instability in thin sheets. Rather than use the optical or potential techniques applied later, india ink was placed at the initial crack front prior to increasing the load [14]. Upon rising load, as the crack started to grow the new material surfaces formed exposed the fluid to vacuum immediately sucking it into the crack tip. The fluid could not follow, however, the crack front as sonic velocities were approached during unstable crack extension. After separation, india ink outlines of the stable slow crack growth region on the fracture surfaces were impressive but later abandoned due to the finding that this promotes stress corrosion cracking or hydrogen embrittlement. As it is clear that this fiducial mark outlines the crack front, this is used in the next section.

SLOW CRACK GROWTH ANALYSIS

The crack tip angle can be measured by scanning with a profilometer across a blister without its removal, and by measuring the crack arrest mark geometry after a blister removal (Figure 12).

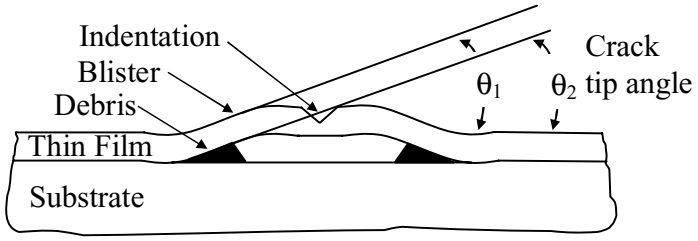

Figure 12. Crack opening displacement angle measurement. θ_1 is the angle measured from the blister angle without its removal, θ_2 is the angle measured from the crack arrest mark geometry.

For the Cu film without a W overlayer and the Ti/Cu/W system, the acoustic energy for the same load was at least two orders of magnitude lower than Cu/W system. As the adhesion of the Cu only versus the Cu/W was identical, the only conclusion here is that the higher available stored elastic energy in the Cu/W system grew the crack relatively rapidly during delamination. This gave an easily detectable event(s) as opposed to the Cu only where the crack must have grown more slowly in many undetectable acoustic events below threshold. The latter is consistent with the more well-adhered Ti/Cu/W system where slow crack growth resulted in many undetectable acoustic events. It is clear then in many cases the crack is growing quite slowly making the Rices Drugan and Sham (RDS) analysis [15] of the tearing modulus an appropriate model to consider. The RDS model of the tearing modulus, T_0, gives [15]:

$$T_0 = \frac{E\delta_c}{\alpha\sigma_{ys}r_m} - \frac{\beta}{\alpha}\ln\left(\frac{e\lambda EJ_0}{r_m\sigma_{ys}^2}\right) \qquad (1)$$

where δ_c/r_m is the crack-tip displacement at a distance r_m behind the crack tip where it is measured or crack tip opening angle (CTOA=δ_c/r_m), $\alpha \approx 1$, $\lambda \approx 0.2$, e is the natural logarithm base, E and σ_{ys} are modulus and yield strength, $\beta = 5.1$ from the mechanics description and J_0 is the initial value of the J integral at crack initiation. Calculation demonstrated that the first term

dominated the second for very high yield strength thin films with toughness less than 100 J/m^2, giving

$$T_0 \approx \frac{E\delta_c}{\alpha\sigma_{ys}r_m} \qquad (1a)$$

Since the steady-state strain energy release rate can be given in terms of the tearing modulus by

$$J_{SS} = J_0 \exp\left(\frac{\alpha T_0}{\beta}\right) \qquad (2),$$

it is seen that combining (1a) and (2) leads to a simple expression for strain energy release rate in terms of the crack-tip opening angle,

$$J_{SS} \approx J_0 \exp\left\{\frac{E \cdot CTOA}{\sigma_{ys}\beta}\right\} \qquad (3).$$

With the fiducial mark representing the crack-tip arrest, we suggest that the mark shape may also represent the CTOA as indicated in Figure 12. That is, if the moisture/hydrocarbons/debris mixture is vacuumed into the crack tip and solidifies, this basically represents an internal replica of the crack tip. As noted in Figure 12, this would represent the CTOA in terms of its height divided by its width. Given the 5 to 15 nm height, this would represent the CTOA in the vicinity of 0.29 to 0.86 degrees.
With an average value of 0.01 radians, a modulus of 120 GPa, a yield strength of 1 GPA and $\beta = 5.1$, one finds:

$$J_{SS} = J_0 \exp\{0.23\} \approx 1.27 J_0 \qquad (3a),$$

which means that during slow crack growth the strain energy release rate has barely increased for this 120 nm thick copper film. This is consistent with Figure 2 which suggests that little if any increase in strain energy release rate over the true surface energy occurs for films less than about a 100 nm thick. While this is highly speculative and based on only several observations of such arrest marks, if this can be proven in further evaluations, it could provide an interesting additional means of assessing film toughness characterization.

CONCLUSIONS

AE analysis of an indentation into a superlayer structure was performed. The energy of a given burst AE event was shown to increase with the rise time. For the thin film system with a Ti underlayer, acoustic emission energy varied inversely proportional to the strain energy release rate. It is proposed that this is due to incremental cracking below the detector threshold. Total AE emission energy was found to be much lower for the system with a Ti underlayer due to improved adhesion. This not only reduced the blister area but also limited the size of incremental crack advance thus reducing the number of detectable acoustic events. Crack arrest marks were found after blister removal with an adhesive tape. The feature geometry is proposed to represent the shape of the crack tip, potentially providing the basis for the crack tip opening displacement angle.

ACKNOWLEDGMENTS

The authors wish to greatly acknowledge support through the Department of Energy under DOE contract DE-FG02/96ER45574. The authors would like to thank Antanas Daugela from Hysitron, Inc. for help with acoustic emission setup, Doug Caldwell and Raul Caretta from the Center for Interfacial Engineering for Auger analysis, and Svetlana Yanina for the AFM assistance, John Nelson, Natalia Tymiak and Donald Kramer for valuable discussions. The assistance of the Microtechnology Laboratory staff at the University of Minnesota is also gratefully appreciated.

REFERENCES

1. A. A. Pollock, Metals Handbook, 9th ed. Vol. 17 (ASM International, 1989, 278-294)
2. T.P. Weihs, C.W. Lawrence, B. Derby, C.B. Scruby, J.B. Pethica, (Mater. Res. Soc. Proc. **239**, 1992) pp. 361-366
3. J. Kameda, R. Ranjan, (Mat. Res. Soc. Symp. Proc. **356**, 1995) pp. 853-858
4. D.F. Bahr, J.W. Hoehn, N.R. Moody, W.W. Gerberich, Acta mater. **45** (12) 5163-5175
5. D. F. Bahr, W.W. Gerberich, J. Mater. Res. **13** (4), pp. 1065-1074 (1998)
6. A.A. Volinsky, N.I. Tymiak, M.D. Kriese, W.W. Gerberich and J.W. Hutchinson, Mater. Res. Soc. Proc. **539**, 1998
7. N.I. Tymiak, A.A. Volinsky, M.D. Kriese, S.A. Downs and W.W. Gerberich, submitted to Met. Trans., 1999
8. W.W. Gerberich, D.E. Kramer, N.I. Tymiak, A.A. Volinsky, D.F. Bahr, and M.D. Kriese, submitted to Acta Met., 1998
9. T. W. Wu, J. Mater. Res., **6**, 1991, p. 407
10. MISTRAS 2001 AEDSP-32/16 User's Manual (Physical Acoustics Corporation, Princeton, NJ 1995)
11. C.B. Scruby, J. Phys. E: Sci Instrum. **20**, 946 (1987)
12. W.W. Gerberich, C.E. Hartbower, Int. J. Fract. Mech. **3**, p. 185 (1967)
13. N.I.Tymiak, M.Li, A.A. Volinsky, Y.Katz, W.W.Gerberich, 1999 MRS Spring Meeting, San Francisco, CA, 1999 (to be published)
14. J.E. Srawley and C.D. Beachem, "Fracture of High Strength Sheet Steel Specimens Containing Small Cracks", ASTM Preprint 80a, Philadelphia (1961) p. 1
15. T.L. Anderson, "Fracture Mechanics: Fundamentals and Applications." (CRC Press, Boston, 1991), p. 219